

# Theme III: Experimental studies concerning steel structures, their elements and their connections

Objektyp: **Group**

Zeitschrift: **IABSE reports of the working commissions = Rapports des commissions de travail AIPC = IVBH Berichte der Arbeitskommissionen**

Band (Jahr): **14 (1973)**

PDF erstellt am: **21.07.2024**

## **Nutzungsbedingungen**

Die ETH-Bibliothek ist Anbieterin der digitalisierten Zeitschriften. Sie besitzt keine Urheberrechte an den Inhalten der Zeitschriften. Die Rechte liegen in der Regel bei den Herausgebern.

Die auf der Plattform e-periodica veröffentlichten Dokumente stehen für nicht-kommerzielle Zwecke in Lehre und Forschung sowie für die private Nutzung frei zur Verfügung. Einzelne Dateien oder Ausdrucke aus diesem Angebot können zusammen mit diesen Nutzungsbedingungen und den korrekten Herkunftsbezeichnungen weitergegeben werden.

Das Veröffentlichen von Bildern in Print- und Online-Publikationen ist nur mit vorheriger Genehmigung der Rechteinhaber erlaubt. Die systematische Speicherung von Teilen des elektronischen Angebots auf anderen Servern bedarf ebenfalls des schriftlichen Einverständnisses der Rechteinhaber.

## **Haftungsausschluss**

Alle Angaben erfolgen ohne Gewähr für Vollständigkeit oder Richtigkeit. Es wird keine Haftung übernommen für Schäden durch die Verwendung von Informationen aus diesem Online-Angebot oder durch das Fehlen von Informationen. Dies gilt auch für Inhalte Dritter, die über dieses Angebot zugänglich sind.

## DISCUSSION LIBRE • FREIE DISKUSSION • FREE DISCUSSION

**An Experimental Study on the Hysteretic Behaviour of Steel Braces under Repeated Loading**

Etude expérimentale sur le comportement hystérique de parois en acier sous charge répétée

Eine experimentelle Studie über das Hysterese-Verhalten von Stahlblech-wänden unter wiederholter Belastung

Shosuke MORINO

Ph. D.

Disaster Prevention Research Institute  
Kyoto University, Japan

**INTRODUCTION** It is well known that braces provide the sufficient strength and rigidity to the structure under the horizontal loading. In Fig. 1, hysteretic load-deflection curves of unbraced and braced frames are shown. In spite of the obvious difference in the shapes of hysteretic loops observed from Fig. 1, the dynamic analysis carried in the present design practice often assumes the multi-linear type of hysteretic load-deflection model for both unbraced and braced frames. This difference is mainly caused by the unique feature of the hysteretic load-deflection characteristics of the brace itself, and it is thus essential to know the real behavior of a bar under repeated axial tension and compression, which should simulate the behavior of the brace involved in a real braced frame.

Investigations on the post-buckling behavior of a bar was initiated in order to obtain the ultimate strength of the truss. Masur<sup>(1)</sup> carried out a theoretical study on the ultimate strength of a simple indeterminate truss. Murray<sup>(2, 3)</sup> described the behavior of a bar with residual deflection under eccentric loading by the elastic action and a plastic mechanism curve, and compared his results with test results of triangular and Warren type trusses. Tests of triangular and Warren type trusses were conducted by Nutt<sup>(4)</sup>, and Neal and Griffiths<sup>(5)</sup> reported an approach to obtain the ultimate strength of a truss. Analysis and test of a simply supported column under pure compression were reported by Paris<sup>(6)</sup>.

Experimental investigations on the behavior of braced frames were done by Wakabayashi, et al<sup>(7)</sup>. Fujimoto, et al.<sup>(8)</sup> showed the results of finite element type numerical analysis of behaviors of braces and braced frames. Igarashi, et al.<sup>(9)</sup> derived the relation between the increments of applied force and deformation of a brace based on a yield condition for a rectangular cross section and flow rule, and analysed the behavior of a brace and braced frame. Nonaka<sup>(10)</sup> obtained an analytical solution for the hysteretic behavior of a centrally loaded steel bar, introducing a plastic hinge at the center which was defined by a linear yield condition of the cross section. Shibata, et al.<sup>(11)</sup> took an approach to the problem in which the deformation distributed along the longitudinal axis of a bar is assumed to be concentrated within a flexural

portion located at the center with a certain length, so that the effect of the partial yield of the cross section could be taken into account. Higginbotham and Hanson<sup>(12)</sup> conducted the analysis including the nonlinear term of the curvature. Yamada and Tsuji<sup>(13)</sup> analysed a bar under repeated axial loading, assuming bi-linear type stress-strain curve and simplifying the section into 3-point model. Very similar experimental study to the one presented in this paper was already conducted by Wakabayashi, et al<sup>(14)</sup>.

**TESTS** Shape and size of a specimen manufactured by shapering SS41 mild steel sheet are shown in Fig. 2. All specimens have square cross section with nominal size 15mm x 15mm, and the value of the length  $\ell$  (Fig. 2) divided by the radius of gyration varies from about 40 to 160. When a specimen is fixed in the loading apparatus described later, rotation axes of the apparatus are to lie at both ends of the length  $\ell$ . Measured dimensions and slenderness ratio are shown in Table 1.  $N_{cr}$  in Table 1 is observed buckling load. Each specimen name listed in Table 1 is composed of two alphabets and numerals. First letter denotes the loading condition; repeated (R) or monotonic (M). Second denotes the position of the load; centric (C) or eccentric (E). Numerals indicate an approximate value of the slenderness ratio. The specimens with the letter R at the end of their names are tested under the different loading program from others, as described later. The eccentricity is given by the formula,  $i/20 + \ell/500$ , where  $i$  is the radius of gyration. Mean values of mechanical properties of the steel material used are shown in Table 2, and a typical stress-strain curve in Fig. 3.

Figure 4 shows the loading apparatus with a deflected specimen. The apparatus is mainly composed of two frames; inner and outer frames. The outer frame is fixed to the cross head or the bed of Autograph universal testing machine, and the inner frame supporting the specimen can freely rotate about the rotation axis at which two frames are connected with no rotational friction by means of thrust and radial bearings.

Starting from the virgin compression, all specimens except RC40R and RC100R are first subjected to a few cycles of alternately repeated axial loading, with relative axial displacement amplitude being controlled at a prescribed value ( $\Delta/\ell = 0.005$ ). After hysteresis loops stabilize, the controlling displacement amplitude is increased by the amount of 0.5% of the specimen length  $\ell$ , and another few cycles of loading are applied. RC40R is first subjected to the virgin tensile loading, and subsequent repeated loading is so applied that only tensile axial displacement occurs. The loading program for RC100R shown in Fig. 23, is determined to investigate the stabilization of the hysteresis loops under the repeated loading with small displacement amplitude, after the specimen experiences the large displacement.

**TEST RESULTS** In Figs. 5-22, test results of the load (N) - relative axial displacement ( $\Delta$ ) and the load (N) - midpoint lateral deflection (V) relationships are shown, referring to Fig. 24. Buckling behaviors of specimens tested under the monotonic loading are shown in Figs. 5-11. Euler loads computed for the specimens which buckled elastically show a good agreement with the experimental buckling loads, and this is believed to guarantee the supporting pin in Fig. 4 worked ideally.

Test results under repeated loading are shown in Figs. 12-22. General behavior of a steel bar under repeated centric axial loading observed from the test can be explained referring to the schematically drawn hysteresis loops in Fig. 25. Under the virgin compression, the bar is shortened keeping its straightness from point O. When it buckles at point A, the sustained load decreases to point B with a very rapid increase of both the axial displacement

and the lateral deflection (point B'). After the loading direction is reversed at prescribed turning point B, the slope of the hysteresis curve at point B is much smaller than the initial elastic slope due to the existence of the lateral deflection. The curve, then, once shows still smaller slope, and proceeds to point D, the slope being steeper. The plastic elongation occurs at point D and the plateau between points D and E corresponds to the plateau of the stress-strain curve of the material. A point which should be noted is that the lateral deflection does not decrease much (points D' to E') even when the load-axial displacement curve shows the plateau, and thus the small lateral deflection remains at the turning point E. Because of this residual lateral deflection, the maximum compressive strength of the bar in the second cycle attained at point G is much smaller than the first one at point A, and sudden buckling action does not appear. After the loading direction is again reversed at point H, the curve goes to point I following nearly the same path with B-C-D. But, the plateau does not appear this time and the maximum tensile strength attained at point I is much smaller than that at point E. The loop in the third cycle is similar to that in the second cycle, and the loop stabilizes after a few cycles of loading.

Regardless the number of the loading cycle, the end of specimen under central loading rotates about the pin axis always in the same direction which is determined at the time of the buckling under the virgin compression. However, in case of eccentrically loaded specimens, the direction of the rotation at the end is reversed when the first tension load is applied right after the buckling occurs under the virgin compression. This phenomenon is exaggerated when the slenderness ratio becomes large.

A test result for RC100R in Fig. 22 under the loading program in Fig. 23 demonstrates the rapid stabilization of the hysteresis loops within the small displacement amplitude ( $\Delta/l = \pm 0.5\%$ ), after the specimen experiences the repeated loading within the large amplitude ( $\Delta/l = \pm 1.0\%$ ).

EXPERIMENTAL OBSERVATIONS The following observations are made.

1. Regardless the axial displacement amplitude, the hysteresis loop stabilizes after 5 to 10 cycles of loading. It seems that the loop of a specimen with larger slenderness ratio stabilizes faster. The loop stabilization of an eccentrically loaded specimen is slightly delayed in comparison with centrally loaded one.

2. When the repeated loading with the small displacement amplitude is applied on a specimen which has already experienced the larger displacement, the hysteresis loop promptly stabilizes (Fig. 22).

3. Once the plastic deformation occurs in a specimen due to the buckling, the lateral deflection does not disappear even when the specimen is subjected to considerable amount of the elongation. The residual lateral deflection measured at zero load tends to gradually increase as the number of loading cycle becomes larger, and thus both maximum tensile and compressive strengths obtained in each cycle of loading under the prescribed displacement amplitude become smaller.

4. The centrally loaded specimen keeps the single-curvature deflected shape resulted from the buckling, during the whole history of loading. On the other hand, two inflection points of the curvature appears near ends of the eccentrically loaded specimen, when the first tensile load is applied after the buckling occurs. This deflected shape is exaggerated in the long specimens.



5. The slope of N- $\Delta$  hysteresis loop at the point at which the load is changed from compression to tension (for example, point C in Fig. 25) becomes smaller, as the number of loading cycle, slenderness ratio and controlling displacement amplitude become larger. The slope of the loop when the load changes from tension to compression is nearly equal to the initial elastic slope, since the effect of the lateral deflection is small.

6. The phenomenon described in the above items 1, 3, 4 and 5 are also observed in the test of RC40R, subjected to the cyclic loading causing only tensile axial displacement (Fig. 21).

7. General observation of the stabilized hysteresis loops of each specimen may derive the conclusion that the compressive load carrying capacity and the hysteretic energy absorbing capacity are not much expected in the case of the long specimen. The most critical point may be that the maximum tensile strength appearing in the stabilized hysteresis loop obtained under a prescribed displacement amplitude is much less than the yield load obtained from the usual tension test.

ACKNOWLEDGEMENT The study presented in this paper was done as a part of the project entitled "Studies on the Elastic-Plastic Behavior of the Steel Braces under Repeated Axial Loading" sponsored by the Ministry of Education, Japan. The head of the project is Prof. Minoru Wakabayashi, Kyoto University. Principal investigators involved in the experimental study are Prof. Chiaki Matsui, Kyusyu University, Messrs. Takeshi Nakamura and Nozomu Yoshida, Kyoto University, including the author. Theoretical investigations are taken part in mainly by Prof. Taijiro Nonaka, Kyoto University, and Prof. Michio Shibata, Osaka Institute of Technology. The author wishes to express his sincere appreciation for the advice, comments and criticisms received from them.

References 10 and 11 have been published in relation to this project, and preliminary investigations prior to this project was reported in Ref. 13.

Acknowledgements are also due Prof. Tsuneyoshi Nakamura, Kyoto University, and Prof. Ryoichi Sasaki, Osaka Technical High School, who kindly offered testing facilities.

#### REFERENCES

1. Masur, E. F.: POST BUCKLING STRENGTH OF REDUNDANT TRUSSES, Proc. ASCE, Vol. 79, No. 332, Oct. 1953, pp. 332-1-14.
2. Murray, N. W.: THE DETERMINATION OF THE COLLAPSE LOADS OF RIGIDLY JOINTED FRAMEWORKS WITH MEMBERS IN WHICH THE AXIAL FORCES ARE LARGE, Proc. ICE, Vol. 5, April 1956, pp. 213-232.
3. Murray, N. W.: FURTHER TESTS ON BRACED FRAMEWORKS, Proc. ICE, Vol. 10, Aug. 1958, pp. 503-516.
4. Nutt, J. G.: THE COLLAPSE OF TRIANGULATED TRUSSES BY BUCKLING WITHIN THE PLANE OF TRUSSES, The Structural Engineer, Vol. 37, May 1959, pp. 141-149.
5. Neal, B. G. and Griffiths, D. M.: THE COLLAPSE OF RIGIDLY JOINTED SINGLY REDUNDANT LIGHT ALLOY TRUSSES, The Structural Engineer, Vol. 41, Dec. 1963, pp. 399-406.
6. Paris, P. C.: LIMIT DESIGN OF COLUMNS, J. Aeronautical Sciences, Vol. 21, No. 1, 1954, pp. 43-49.
7. Wakabayashi, M. and Tsuji, B.: EXPERIMENTAL INVESTIGATION ON THE BEHAVIOR OF FRAMES WITH AND WITHOUT BRACING UNDER HORIZONTAL LOADING, Bulletin, Disaster Prevention Research Institute, Kyoto University, Vol. 16, Part 2, Jan. 1967, pp. 81-96.
8. Fujimoto, M. et al.: NONLINEAR ANALYSIS FOR K-TYPE BRACED STEEL FRAMES,

- Transaction, Architectural Institute of Japan, No. 209, July 1973, pp. 41-51 (in Japanese).
9. Igarashi, S., et al.: HYSTERETIC CHARACTERISTICS OF STEEL BRACED FRAMES, Transaction, Architectural Institute of Japan, No. 196, June 1972, pp. 47-54 (In Japanese).
  10. Nonaka, T.: AN ELASTIC-PLASTIC ANALYSIS OF A BAR UNDER REPEATED AXIAL LOADING, Int. Jour. Solids and Structures, Vol. 9, No. 5, May 1973, pp. 569-580.
  11. Shibata, M., et al.: ELASTIC-PLASTIC BEHAVIOR OF STEEL BRACES UNDER REPEATED AXIAL LOADING, Preprint, 5th WCEE, Rome, 1973, No. 100.
  12. Higginbotham, A. B. and Hanson, R. D.: INELASTIC CYCLIC BEHAVIOR OF AXIALLY-LOADED MEMBERS, Presented at Annual Meeting of CRC in Chicago, Mar. 1972.
  13. Yamada, M. and Tsuji, B.: ELASTO-PLASTIC BEHAVIOR OF BRACINGS UNDER THE CYCLIC AXIAL FORCES (PART I), Transaction, Architectural Institute of Japan, No. 205, March 1973, pp. 31-35 (in Japanese).
  14. Wakabayashi, M., et al.: AN EXPERIMENT ON THE BEHAVIOR OF A STEEL BAR UNDER REPEATED AXIAL LOADING, Annuals, Disaster Prevention Research Institute, Kyoto University, No. 14A, April 1971, pp. 371-381 (in Japanese).

**FIGURES AND TABLES**

**Table 1 Size of Specimens**

SPECIMEN NAME	LENGTH (cm)	WIDTH (mm)	DEPTH (mm)	SLENDERNESS RATIO	$N_{cr}$ (t)
MC 40	19.37	14.97	15.01	44.70	5.82
MC 80	36.78	15.01	15.05	84.67	5.22
MC 120	54.01	14.97	15.03	124.48	3.17
MC 160	71.39	14.95	15.02	164.64	1.93
ME 40	19.39	14.97	15.04	44.65	5.10
ME 80	36.70	15.00	15.03	84.47	3.67
ME 120	54.01	15.00	15.03	124.48	2.29
RC 40	19.50	15.06	15.08	44.80	6.23
RC 40R	19.33	14.96	15.09	44.43	5.25
RC 60	27.99	14.99	15.03	64.51	5.94
RC 80	35.65	15.05	14.95	85.43	5.49
RC 100	45.32	15.01	15.06	104.26	3.60
RC 100R	45.29	15.01	15.04	104.31	2.60
RC 120	54.05	14.99	15.02	124.65	3.72
RC 160	71.33	15.01	15.03	164.39	2.32
RE 40	19.29	14.98	15.06	44.38	5.29
RE 80	36.67	15.01	15.03	84.51	3.81
RE 120	54.01	14.99	15.03	124.48	2.58

**Table 2 Mechanical Properties**

YOUNG'S MODULUS	$2.18 \times 10^3 \text{ t/cm}^2$
YIELD STRESS	$2.55 \text{ t/cm}^2$
ULTIMATE STRENGTH	$4.37 \text{ t/cm}^2$
STRAIN-HARDENING STRAIN	1.3 %
EXTENSIBILITY	31.8 %
STRENGTH OF RUPTURE	$3.15 \text{ t/cm}^2$

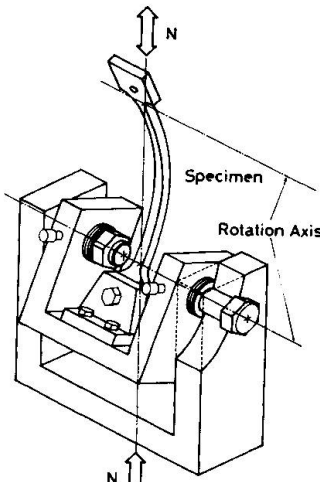


**Fig. 4 End Support**

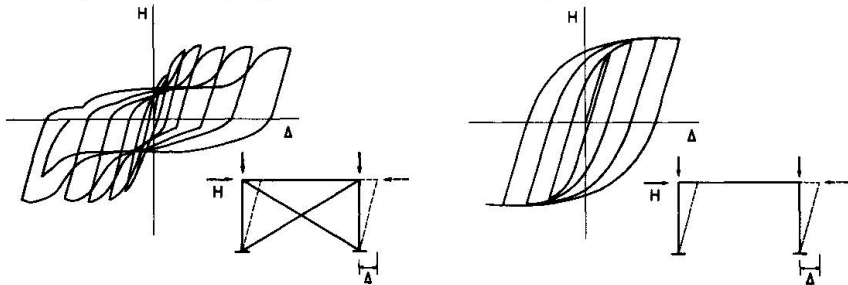


**Fig. 1 Hysteresis Loops of Braced and Unbraced Frames**

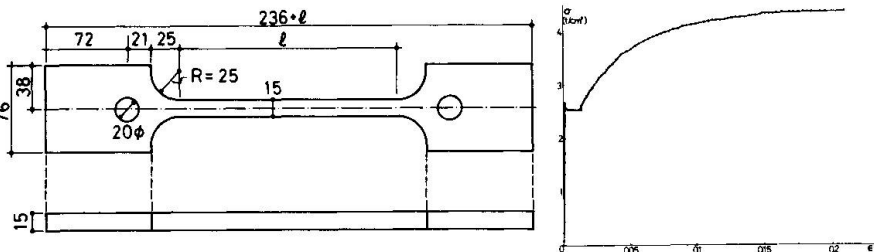


**Fig. 2 Test Specimen**

**Fig. 3 Stress-Strain Curve**

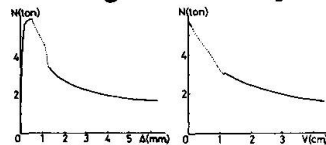


**Fig. 5 MC40**

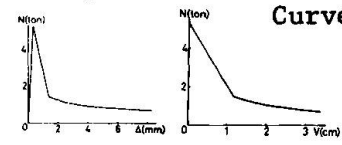


**Fig. 6 MC80**

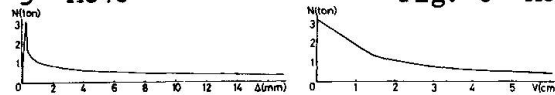


**Fig. 7 MC120**

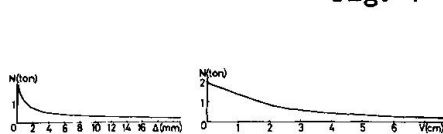


**Fig. 8 MC160**

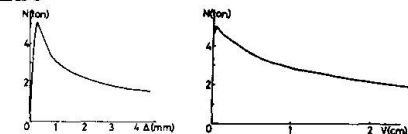


**Fig. 9 ME40**

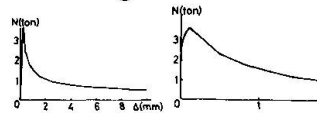


**Fig. 10 ME80**

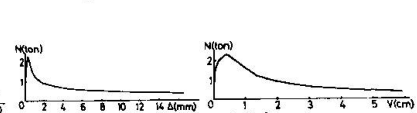


**Fig. 11 ME120**

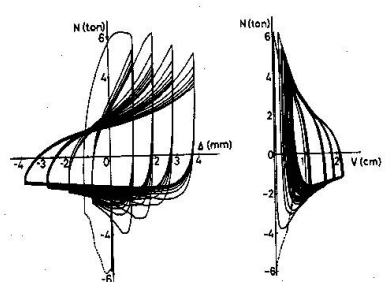


Fig. 12 RC40

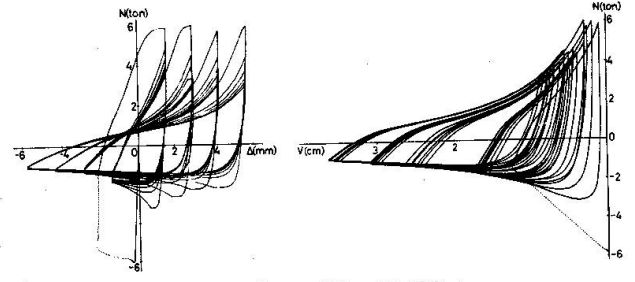


Fig. 13 RC60

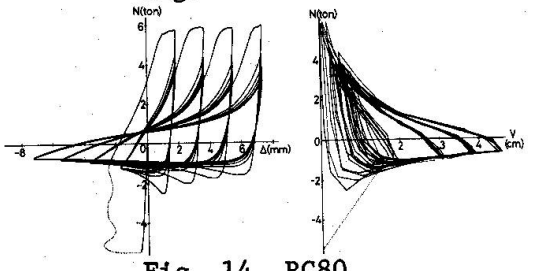


Fig. 14 RC80

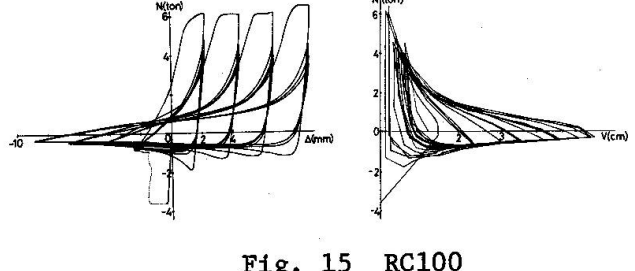


Fig. 15 RC100

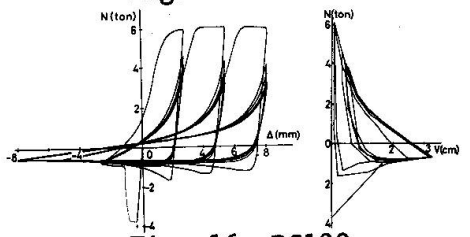


Fig. 16 RC120

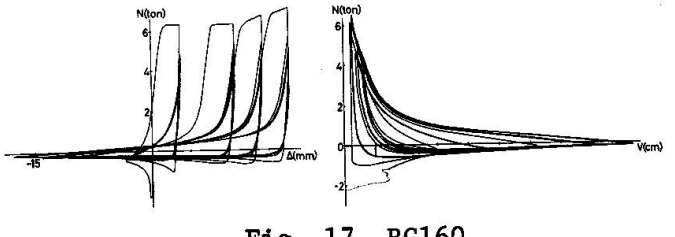


Fig. 17 RC160

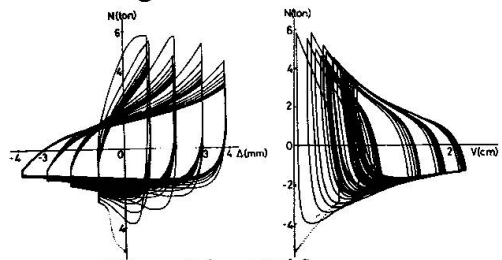


Fig. 18 RE40

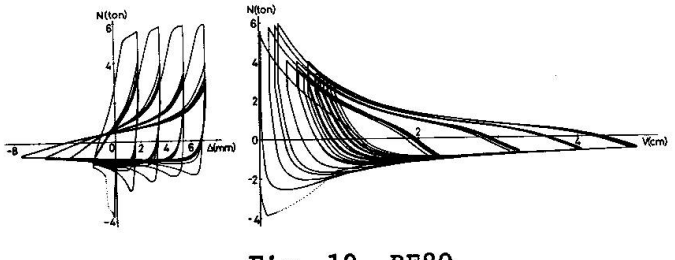


Fig. 19 RE80

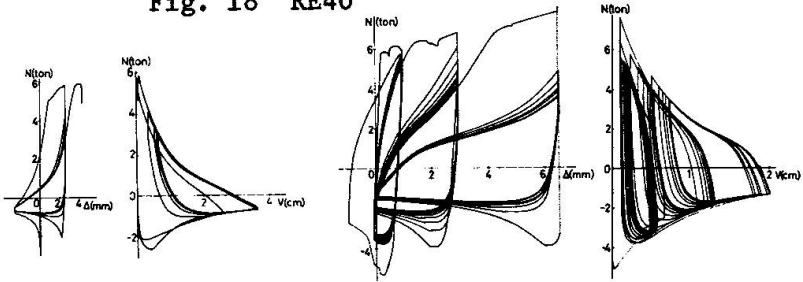


Fig. 20 RE120

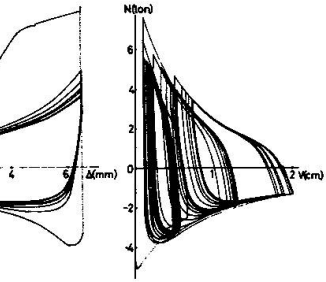


Fig. 21 RC40R

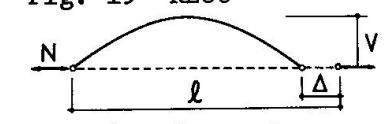


Fig. 24 Deformations

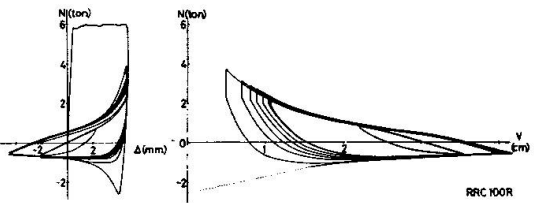


Fig. 22 RC100R

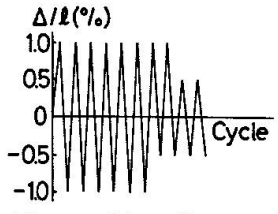


Fig. 23 Loading Program for RC100R

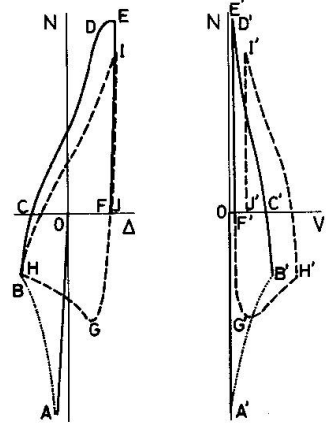


Fig. 25 Schematic Hysteresis Loops

## SUMMARY

An experimental study is carried out in order to investigate the hysteretic behavior of steel braces subjected to repeated axial tension and compression. In the test program, all specimens of SS41 mild steel bar simply supported at both ends have an identical cross section with a nominal dimension 15 mm x 15 mm, and slenderness ratio varies from about 40 to 160. The repeated axial load is applied centrally or eccentrically on the specimen through the loading apparatus which assures free rotation at both ends of the specimen, under the loading program that controls the relative axial displacement at a prescribed value until the hysteresis loop stabilizes after a few cycles of loading. The loop stabilization, effects of slenderness ratio on the shape of the loop and effects of residual deformation on the load carrying capacity of the bar are discussed based on the experimental results.

## RESUME

On étudie par voie expérimentale le comportement de l'hystérésis de parois minces en acier soumises à des tensions et compressions axiales. Dans le programme d'essai toutes les éprouvettes en acier doux SS41 appuyées aux deux extrémités ont la même section de 15 x 15 mm et un degré d'allongement d'environ 40 à 160. La charge axiale répétée est appliquée centriquement et excentriquement sur l'éprouvette moyennant l'appareil de charge permettant la rotation libre aux deux extrémités de l'éprouvette. Elle est exercée sous le programme de charge contrôlant le déplacement relatif axial à une valeur prescrite jusqu'à stabilisation de la boucle d'hystérésis après quelques cycles de charge. La stabilisation de la boucle, l'effet d'allongement sur la forme ainsi que l'effet de la déformation résiduelle sur la capacité de charge de l'éprouvette sont discutés sur la base des résultats expérimentaux.

## ZUSAMMENFASSUNG

Es wird eine experimentelle Studie zur Erforschung des Hysterese-Verhaltens von Stahlblechwänden durchgeführt, die wiederholter axialer Spannung und axialem Druck ausgesetzt sind. Im Versuchsprogramm besitzen alle, an beiden Enden einfach gelagerte Probestäbe aus Flusstahl SS41 gleichen Querschnitt von 15 x 15 mm und einen Schlankheitsgrad von ca. 40 bis 160. Die wiederholte axiale Belastung wird zentrisch oder exzentrisch auf den Probestab mittels des Belastungsapparates ausgeübt, der die freie Drehung an dessen Enden gestattet. Sie erfolgt unter dem Belastungsprogramm, welches die relative Axialverschiebung bei einem vorgeschriebenen Wert kontrolliert, bis sich die Hystereseschleife nach einigen Belastungszyklen stabilisiert. Die Schleifenstabilisierung, die Wirkung des Schlankheitsgrades auf die Form der Schleife sowie der Effekt von Restdeformation auf die Belastungskapazität des Stabes werden aufgrund der experimentellen Ergebnissen diskutiert.

Leere Seite  
Blank page  
Page vide

**Incremental Collapse of Thin Webs subjected to Cyclic Concentrated Loads**

Rupture des âmes minces soumises à des charges cycliques concentrées

Kollaps von dünnen Stegen unter zyklischer Belastung durch Einzellasten

**Allan BERGFELT**  
 Professor, Structural Engineering  
 Steel and Timber Structures  
 Chalmers University of Technology  
 Göteborg, Sweden

Some comments and complements are here given to the problem treated in the paper by P. Novák and M. Škaloud [1] on the above subject.

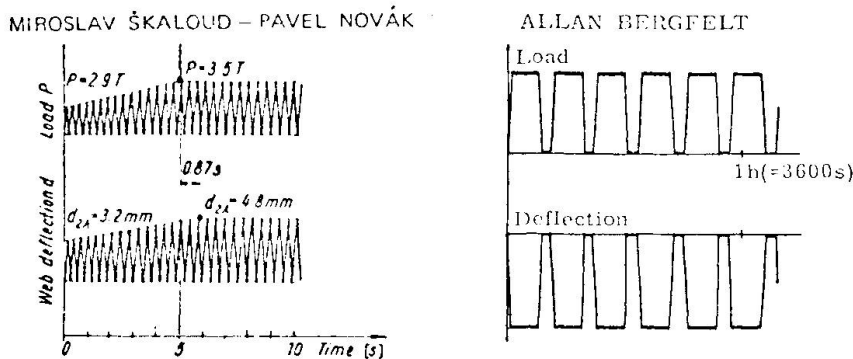


Fig.1. Different shape of loading cycles.

The authors have performed tests, where the maximum load in every cycle has been attained during a very short time only, fig.1. In each cycle, load values causing plastic deformations, seem to have been kept during a few hundredths of a second only, in the "fast" cycles, or during a few seconds in the "slow" cycles. In my tests the maximum load has been kept for several minutes in every cycle as is illustrated by fig.1.

My test results agree, in principle, with those of Novák and Škaloud (except for the girders with very small flange stiffness factor). That is, the reduction of the load carrying capacity caused by repeated loading was



found to be very small. In figure 2 the failure loads after 2 cycles – circular points – or after many cycles (up to about 1000) – triangular points – are plotted against the flange-to-web thickness ratio. The failure loads are divided by web crippling load under monotonously increasing loading. These failure load ratios are very close to 1, although in most cases a little less than 1,0. Even the lowest ratios are not less than 85 à 90 %, which I have reported earlier [2].

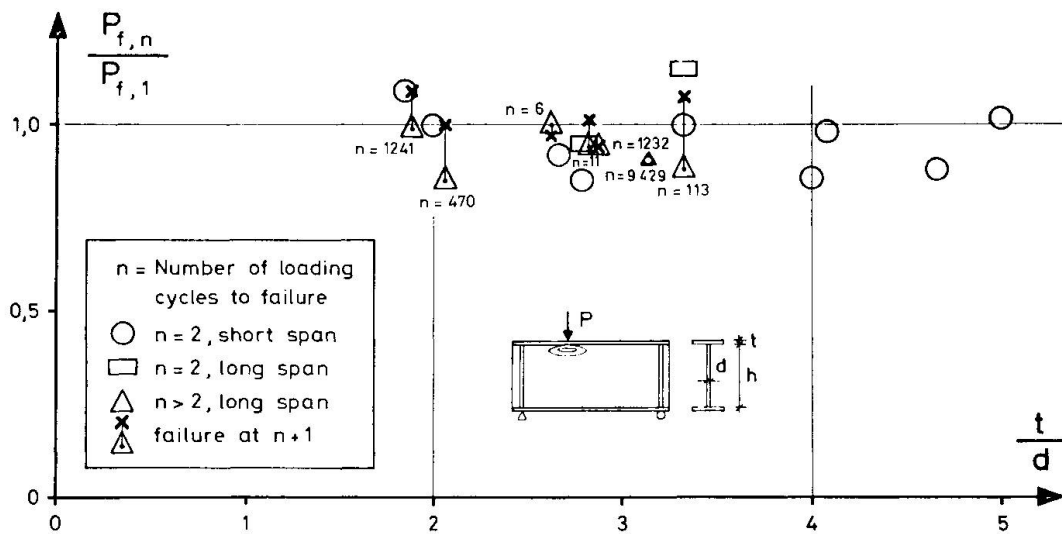


Fig.2. Ratios of failure load under repeated loading to failure load under monotonous loading.

As usual the greatest difference in deformation is measured between the first and second loading. A repeated loading that goes on for hundreds of cycles causes only a slight further increase. From these tests it was hard to find any difference in failure load between the 2 cycle tests and the tests with up to about 1000 loading cycles. Of course the scatter of the results is rather great, depending on initial deformations and initial stresses.

One test was however performed to about 10 000 loading cycles with a maximum load of 90 % of the foreseen crippling load under monotonously increasing loading. Here a crack appeared in the web after about 5000 cycles. The crack was mainly horizontal and about 3 cm below the flange right under the load with slightly bents upwards at each side until a total length of about 10 cm. No significant increase of vertical deformation was observed. Nothing more happened during the following 4 000 loading cycles than that the length of the crack increased to about 20 cm. Soon thereafter at 9 429 cycles a buckling failure occurred. The girder was of

ordinary carbon steel with a yield stress  $\sigma_y \approx 3300$ . Flange 18 x 350 mm, web 6 x 700 mm. Max. load 31,5 tons was for the somewhat shortened cycles of just this test, held during nearly 30 sec. in every cycle. The max. vertical stress was about 3000 kp/cm<sup>2</sup> and the breathing under the loading cycles caused bending strains of similar magnitude. The crack was visible on both sides of the web. Its maximal width was largest on one side at max. load and on the other side at unloading.

The local crack demonstrates that even if the girder can bear a certain load in one point during many cycles, this repeated load will cause a collapse if it is movable along the span.

\*

The most important new results in my investigation is however that girders both of ordinary carbon steel and of high strength steel have been tested [3]. The results for high strength steel are in fig. 3 marked with filled dots (or partly filled dots).

It is seen - which is quite obvious - that the girder can carry higher concentrated loads when the yield point of the steel increases. (This is true also for such a hybrid girder with high strength steel in the web only). It is also seen that the increase of failure load is not directly proportional to the yield stress which is quite normal as buckling is dominating. The lines of the diagram illustrates what in the case of direct proportionality should have been expected for an ordinary steel with yield points of  $\sigma_y = 2000$  or 3000 and a high strength steel of 6000 kp/cm<sup>2</sup>. It is seen that for example the filled dots for 6000 kp/cm<sup>2</sup> fall much below the corresponding theoretical line. The failure loads seem to be approximately proportional to  $\sqrt{\sigma_y}$  (or still better to  $\sigma_y^{2/3}$ ) and not directly proportional to  $\sigma_y$ . Of course this concerns only those tests where  $t/d \gtrsim 2$  and thus buckling is dominating.

In a diagram (fig. 4) where the load is divided by  $\sqrt{\sigma_y}$  the results for different steel qualities fall rather near the theoretical lines. (As is pointed out in [2] the flange thickness  $t$  ought to be corrected to  $t_1 = t\sqrt[4]{b/25t}$ , which is however not done in this discussion report).

Of special interest for this symposium are the results for repeated loads. These points are marked with dots completed with two small upward

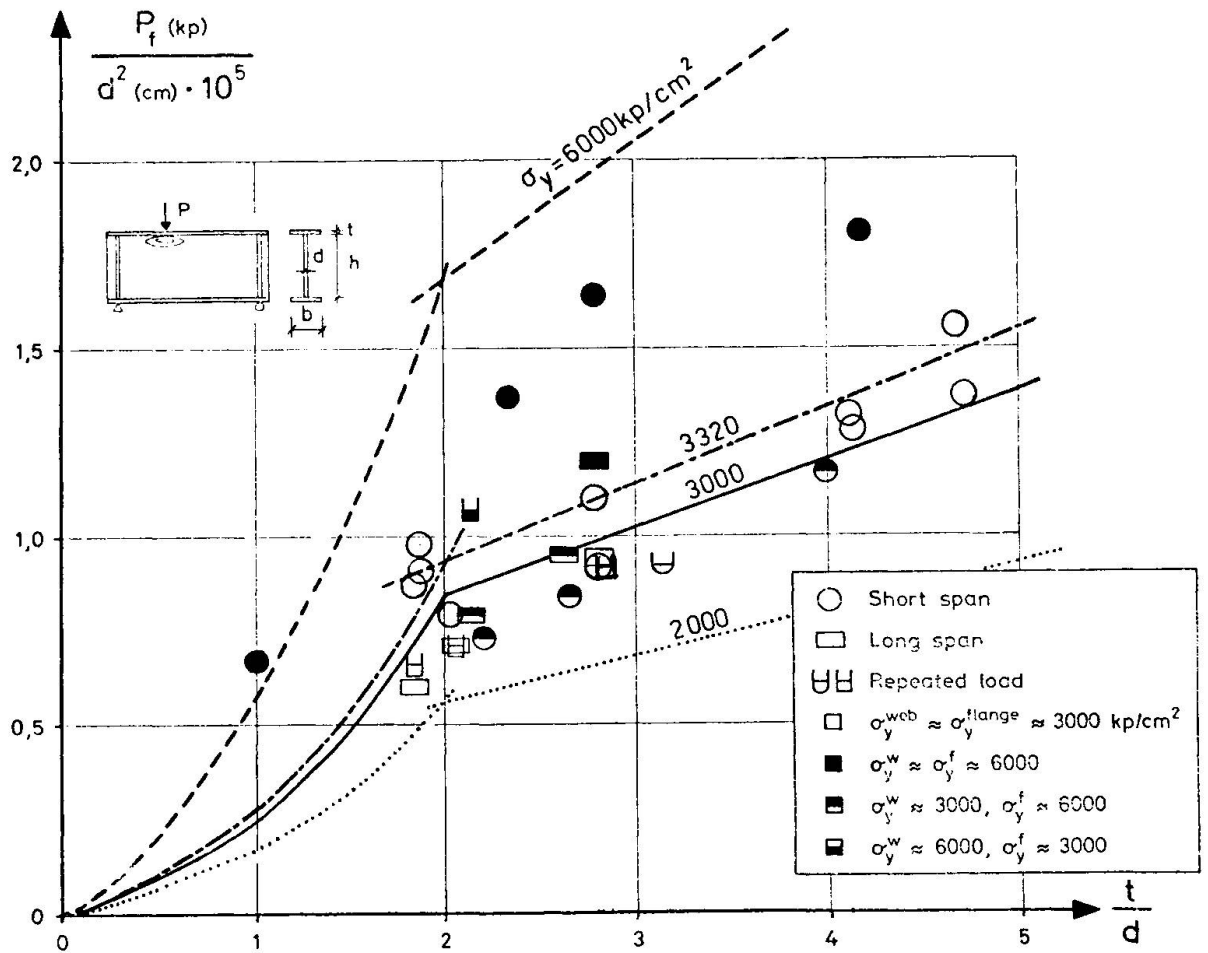


Fig.3. Failure loads (crippling) for different steel qualities.

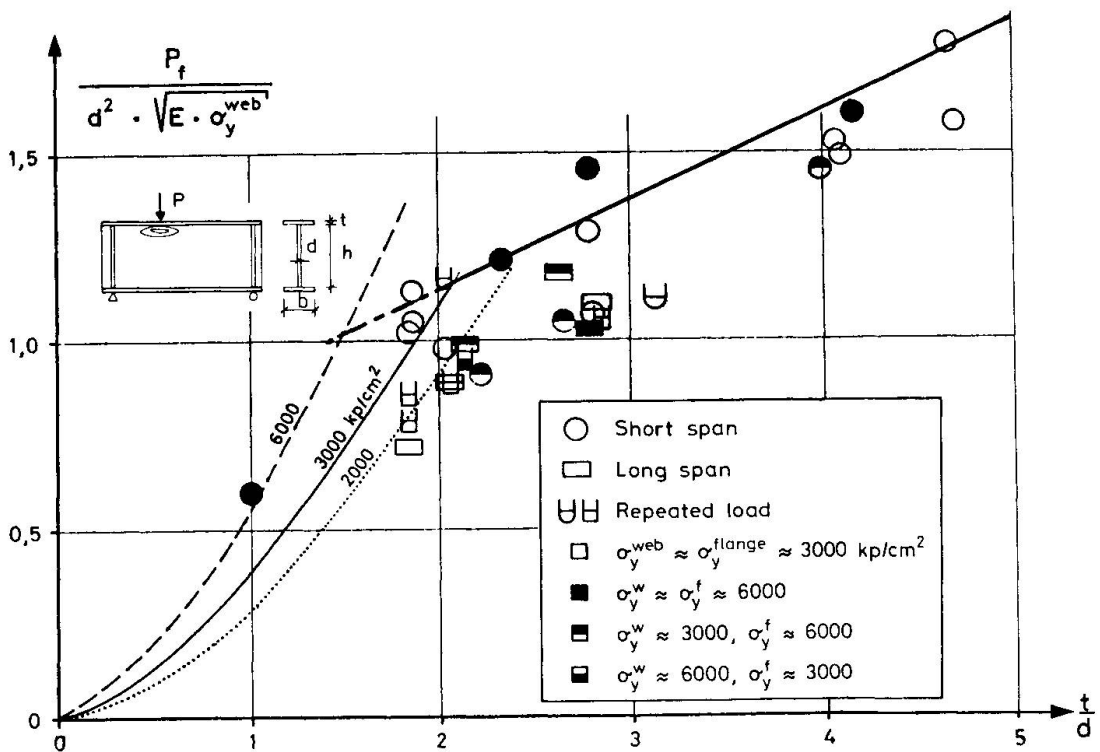


Fig.4. Failure load (crippling) divided by  $\sqrt{\sigma_y}$  and for different steel qualities.

lines. It is seen that also these results fall within the scatter region. The points fall, however, generally in the lower part of this region.

\*

#### References :

- [ 1 ] P. Novák - M. Škaloud : Incremental collapse of thin webs subjected to cyclic concentrated loads. IABSE Symposium Lisboa 1973, Preliminary report p.179.
- [ 2 ] A. Bergfelt : Post-buckling behaviour of webs under concentrated loads. IABSE, Ninth Congress, Amsterdam 1972, Final report p.83.
- [ 3 ] A. Bergfelt - S. Lindgren : Livintryckning vid slanka I-balkar vid upprepad belastning och speciellt vid höghållfast stål (Web crippling for repeated loadings and specially for high strength steel). Nordiske Forskningsdager for Stålkonstruksjoner, Oslo 1973. Rapport II.2/4.

#### SUMMARY

The new test values according to Škaloud and Novák [1] for local web crippling under a concentrated load, are compared to values from tests with loading cycles where the loading period is rather long.

Both static and repeated loadings have been made with girders both of ordinary carbon steel and of high strength steel. Previously given dependance on flange-to-web thickness ratio is completed with the dependance on the yield stress.

#### RESUME

Les résultats d'essais selon Škaloud et Novák [1] concernant la ruine locale de l'âme soumise à une force concentrée variant périodiquement sont comparés à ceux avec des périodes de charges assez longues.

Des essais statiques et avec des charges périodiques ont été réalisés sur des poutres en acier normal et en acier de haute résistance. La dépendance du rapport entre l'aile et l'âme donnée auparavant est complétée par la dépendance de la limite d'élasticité.

#### ZUSAMMENFASSUNG

Die Versuchsergebnisse nach Škaloud und Novák [1] für lokales Stegblechbeulen unter periodisch variierender Einzellast werden mit Ergebnissen unter Wechsellasten mit langer Zeitdauer verglichen.

Die Balken wurden mit statischer Einzellast und mit Wechsellasten geprüft. Sie waren sowohl aus normalem Stahl als aus hochfestem Stahl gefertigt. Die früher gegebene Abhängigkeit der Flanschdicke von der Stegdicke wird hier durch die Abhängigkeit von der Fließgrenze vervollständigt.

Leere Seite  
Blank page  
Page vide

**Shake down Tests on Steel Beams with Distributed Loads**

Essais de shake down sur poutres en acier avec charge répartie

Shake-down-Versuche an Stahlbalken mit verteilter Last

**Germund JOHANSSON**

Tekn. lic.

Chalmers University of Technology

Göteborg, Sweden

Introduction

At Chalmers University of Technology a number of shake down tests have been made on continuous two and three span rolled steel beams.

Testing procedure

The loading scheme of the two span beams is shown in fig.1. The load control and the registration of strain and deflection were arranged to be automatical. In fig.2 the load versus time relationship is shown. The period of a complete load cycle was chosen to either 5 or 10 minutes. For some beams recently tested a cycle period of 20 minutes was used.

The distributed loads were simulated by several (6 or 9) hydraulic jacks per span. Three beams with one or two concentrated loads per span have also been tested.

The span length of the tested beams was 2, 3 and 4 m. The test beams were of European standard HE 100 A, HE 100 B (wide flange beams with about 100 mm depth) and HE 160 A, HE 160 B (wide flange beams with about 160 mm depth). Four beams (no.21-24) were made of two parts (HE 100 A and HE 100 B) butt jointed 0,5 m from the central support. Further data are found in table 1 together with calculated and measured shake down loads.



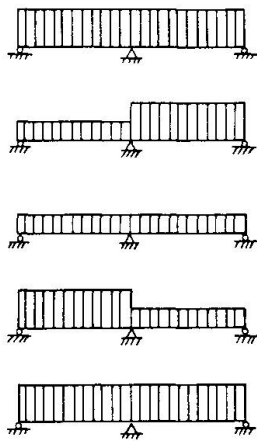


Fig.1 Loading scheme for the two span beams

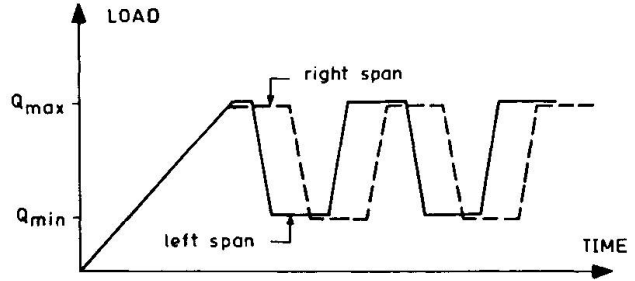


Fig.2. Load versus time relationship

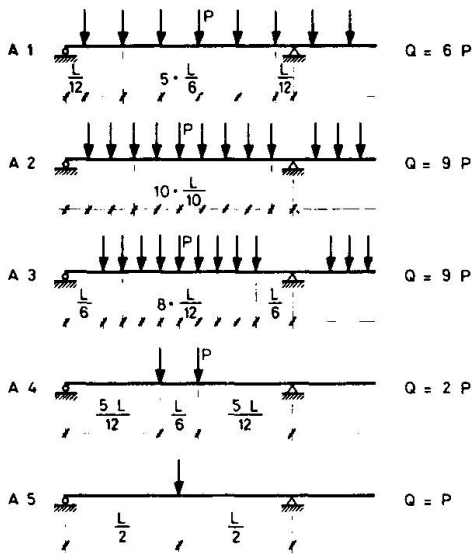


Fig.3 Placing of the hydraulic jacks, cf tab.1

In fig. 4 and 5 some test results are shown. The first diagram shows for a two span beam the measured strain at the central support versus cycle number and the second diagram shows measured midspan deflections of both spans. This beam was retested four weeks later and the measured strain at the central support is shown in fig.5. Notice that in this second test of the same beam greater loads are needed in order to get permanent deflections. Further results are shown in fig. 6 (beam 24). The tendency of stabilization is very clear.

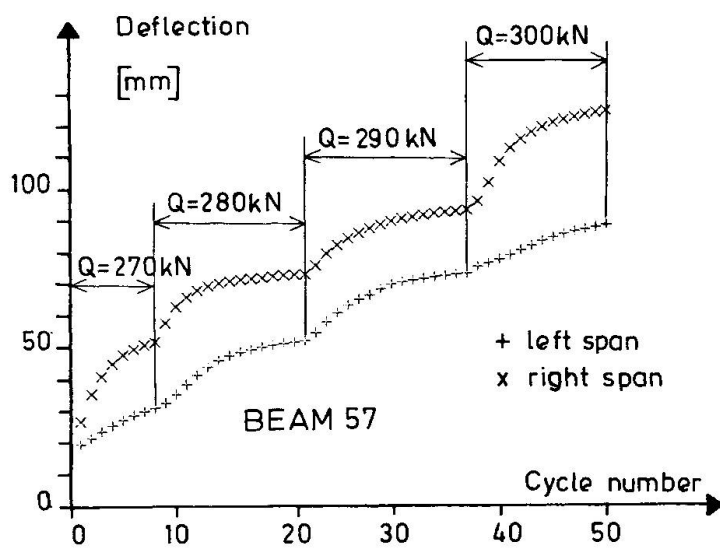
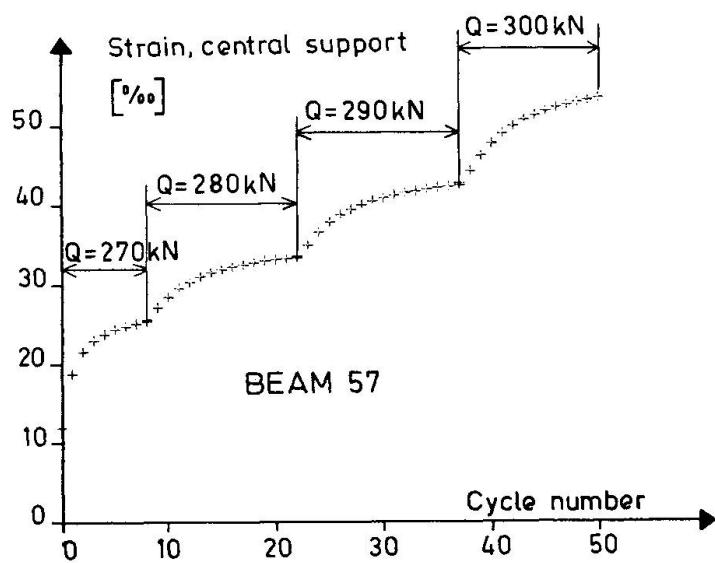


Fig. 4 Measured strain at the central support and measured midspan deflections versus cycle number. Beam 57.

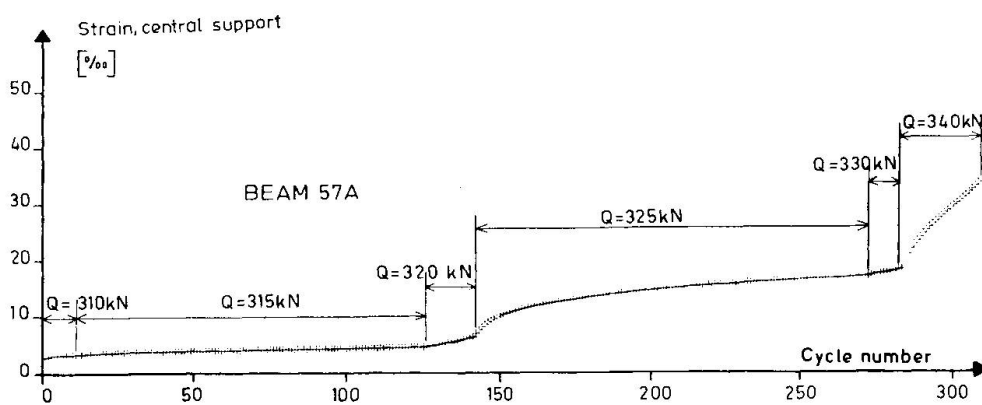


Fig. 5 Measured strain at the central support versus cycle number. Beam 57 A.

### Test results

The tests are not yet fully evaluated, but some results will be given below.

1. Due to strain hardening the measured shake down loads are about 15 % greater than the calculated loads.  
In the tests the shake down loads were found to be almost equal to the calculated plastic loads without regard to shake down.
2. The shake down behaviour is time dependent. To reach a stable behaviour a greater number of load cycles were needed when the time per load cycle was short than when the cycle time was long.  
Further, if the beam is allowed to rest for some time (a rest of four weeks or more has been tested), the shake down load of the retested beam will be greater than at the first test.
3. A few cycles of overloading have a reinforcing effect. Let  $Q_s$  denote the shake down load determined with increasing load levels in the ordinary testing procedure. If the structure then is subjected to some load cycles with a load greater than  $Q_s$ , this will accelerate the stabilization process when the beam is again subjected to the load  $Q_s$ .

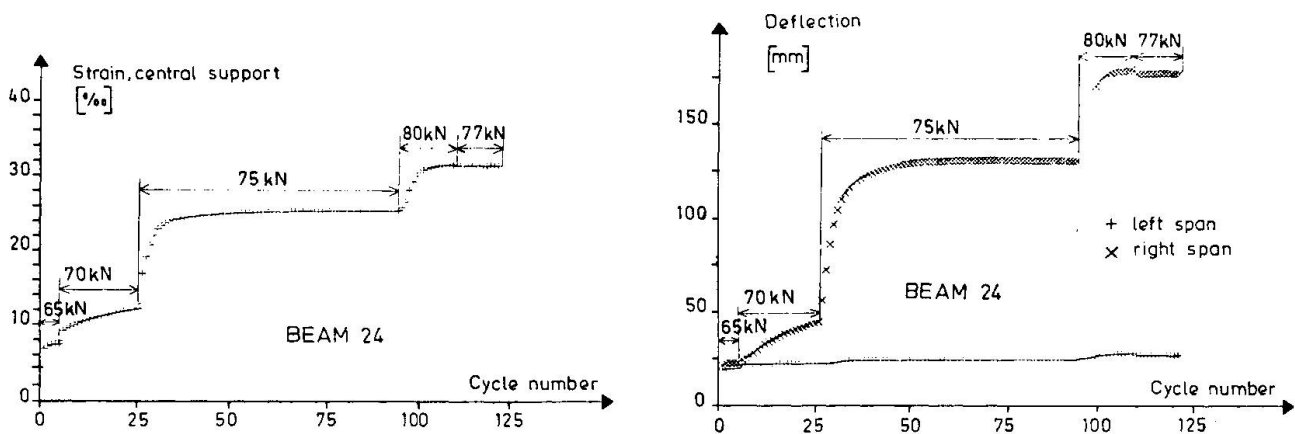


Fig. 6. Measured strain at the central support and measured midspan deflections versus cycle number. Beam 24.

Tab.1 Two span beams

Beam no.	Span length m	Beam	Minutes per cycle	Total number of cycles	Loads (kN)		
					Minimum load	$Q_s^{calc}$	$Q_s^{meas}$
21	3,0	HE100A, B	5	47	30	75	85
22	3,0	HE100A, B	5	35	30	80	> 90
23	3,0	HE100A, B	10	381	15	72	92
24	3,0	HE100A, B	10	121	15	65	80
31	2,0	HE100A	5	85	45	108	135
33	2,0	HE100B	5	95	55	121	150
35	2,0	HE100B weak axis	5	52	30	64	> 80
41	3,0	HE100A	10	32	30	67	> 80
43	3,0	HE100B	10	49	40	95	> 110
44	3,0	HE100B	10	215	20	90	90
45	3,0	HE100A	10	135	15	65	77
52	4,0	HE160A	10	22	60	158	170
53	4,0	HE160B	10	44	80	204	230
55	3,0	HE160A	10	42	30	151	> 175
56	3,0	HE160A	5	73	30	151	175
57	3,0	HE160B	10	50	50	258	> 300
57A	3,0	HE160B	10	309	50	258	320
58	3,0	HE160B	5	67	50	258	> 300
61	3,0	HE160A	5	48	$Q_{max}/3$	130	> 160
63	3,0	HE160B	5	75		183	210
72	3,0	HE160B	5	112		187	215

## SUMMARY

Some results from shake down tests on steel beams are given. The shake down loads were found to be approximately 15% greater than the calculated loads. Further, the time dependence and the effect of an overload are discussed.

## RESUME

On donne quelques résultats d'essai du "Shake down" sur des poutres en acier. Les charges du Shake down s'avéraient de 15% supérieures aux charges calculées. On discute en outre la dépendance du temps et l'effet d'une surcharge.

## ZUSAMMENFASSUNG

Es werden einige Ergebnisse von "Shake-down"-Tests an Stahlbalken mitgeteilt. Die Shake-down-Belastungen erwiesen sich als ungefähr 15% höher als die berechneten Belastungen. Ferner werden die Zeitabhängigkeit und die Wirkung einer Ueberlast diskutiert.

Leere Seite  
Blank page  
Page vide

### III

#### Summary Report on Theme III

Rapport sommaire au thème III

Zusammenfassender Bericht zum Thema III

**Ben KATO**

Professor of Structural Engineering  
University of Tokyo  
Tokyo, Japan

The primary results to be extracted from the discussions to Theme III are to obtain a method to predict the deformation response of steel structures and their elements against well-defined, nonstationary repeated and reversed loading and to find the maximum strength and deformation for such loading, rather than the evaluation of fatigue strength and phenomenological description of cyclic behaviour.

In the analysis of frames and members for which buckling is not critical, it seems to be best, as Dr. Popov pointed out, to start with a stress-strain diagram obtained for cyclic loading. This is then integrated to obtain the moment-curvature relation for a given member section. Finally, using the latter information, calculation of the load-deflexion response due to cyclic loading is made. Dr. Akiyama presented such a method for construction of stress-strain diagram of steel material under nonstationary cyclic loading directly from a monotonic stress-strain curve. Using this basic relation, Kato presented in the session of Theme I a method to obtain the load-deflexion response of members and frames under cyclic loading. Dr. Nakamura's remarks were also in the same direction. Each smooth piece of hysteresis loops was approximated by a Ramberg-Osgood equation, and the moment-curvature relation was calculated for a simplified two-parallel flange section. Dr. Popov, in his research, started with the moment-curvature relation obtained from experiments. Dr. Yamada et al. carried out repeated and reversed horizontal loading tests of unit rectangular steel rigid frames. Dr. Igarashi et al. presented test results of beam-columns subjected to repeated and reversed loading under a constant axial thrust. The former assumed a tri-linear and the latter assumed a bi-linear type of stress-strain relationship in their analyses.

Dr. Johansson carried out shake down tests on two span beams. The shake down loads were found to be approximately 15% greater than the calculated loads due to strain-hardening. It was also shown that the shake down behaviour was time dependent.

Six papers dealt with the topics of incremental collapse, repeated loads were applied in post buckling state. Dr. Davies carried out tests of axially loaded continuous beams subjected to both static and cyclic transverse loading. He pointed out that for a structure which



exhibits instability, an incremental collapse would be caused by cyclic loading. Balancing between strain-hardening effect and  $P-\Delta$  effect is a most critical factor in the response to cycles of load. Dr. Morino presented test results of centrally and eccentrically loaded struts. Alternate compressive force and tensile force were applied, while axial displacements were controlled to keep a constant magnitude from each load-free state. In these tests, buckling took place during the compressive loading phase. It was shown that residual lateral deflexion increased and load carrying capacity decreased in each cycle of loading.

Dr. Novák et al. carried out local web crippling tests subjected to repeated concentrated load, and concluded that the cyclic loading and incremental collapse did not lead to any significant reduction in ultimate strength, and consequently, to any premature failure of the girder. Similar tests with rather long cyclic loading period were performed by Dr. Bergfelt. His test results agreed, in principle, with those of Dr. Novák. The most important result in his investigation was that for girders of high strength steel the increase of failure load was not directly proportional to the yield stress but was approximately proportional to the square root of the yield stress.

Dr. Popov demonstrated that beams subjected to cyclic loading can maintain stable loops even after local buckling of flanges has taken place if the beams were sufficiently braced laterally. On the contrary, Dr. Takanashi et al. carried out beam tests without any lateral supports. Due to the occurrence of lateral buckling, reduction of beam stiffness was observed in each cycle of bending, and loops could not attain a stable state. Rotation capacity of a beam under such a cyclic loading condition is considerably lower than that for monotonic loading condition.

Concerning with structural connexions, Dr. Igarashi et al. carried out cyclic bending tests of a beam spliced by high strength bolts. Behaviour of beam-to-column joint panels was reported by Dr. Popov.

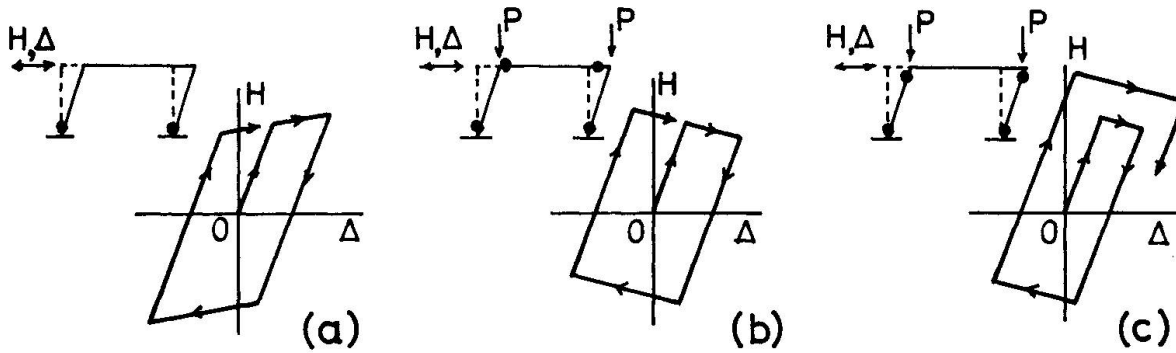
Mr. Takahashi et al. investigated the cyclic behaviour of steel shear walls stiffened transversely as well as longitudinally to form a grid shape. Stable hysteresis loops were obtained when stiffeners were strong enough to allow the wall plate to form a tension field in the post buckling region.

The objective of experimental studies is that the results obtained from those experiments should be digested and integrated into unified formulations which are simple enough for the practical design use. Toward this purpose, the following subjects should be kept in mind:

- The experiments should be planned and carried out in a well coordinated way.
- A prevailing rule derived from experimental results should be checked by the theory pertaining to the phenomenon. In this sense, contents involved in Theme III and those involved in Thems I should be examined and criticized each other. A good example of this can be given. For the behaviour of frames subjected to repeated and reversed horizontal loading, the above figures were obtained experimentally(1), while the figures below were obtained from theoretical basis(2). In the experimental phase, it is difficult to cover all relevant parameters and conclusions might have been drawn from results of a limited number of test specimens.
- Application of the numerical analysis is coming up to follow the experimental behaviour of structures. However this approach does not seem as effective for obtaining general information on the behaviour of structures for a specified loading condition, thus, for the derivation of a practical design formula. In the experimental and theoretical approaches as well, more effort should be made to have an insight into fundamental characteristics of the structural system.

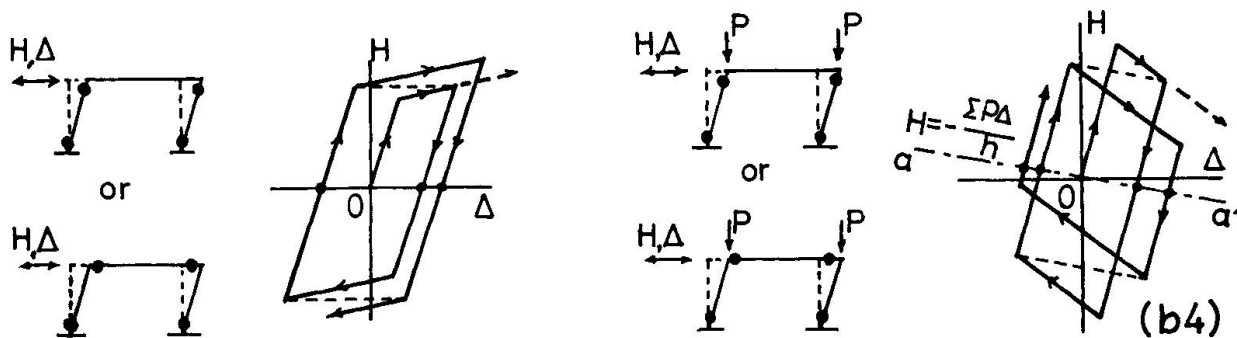
(REFERENCES) (1) Fujimoto, M. and Naka, T., Introductory Report, III, Experimental Studies concerning Steel Structures, their Elements and their Connections, P.56.

(2) Kato, B. and Akiyama, H., Preliminary Report, I, Theoretical Prediction of the Load-Deflexion Relationship of Steel Members and Frames, p.27. (SYMPOSIUM, 1973)



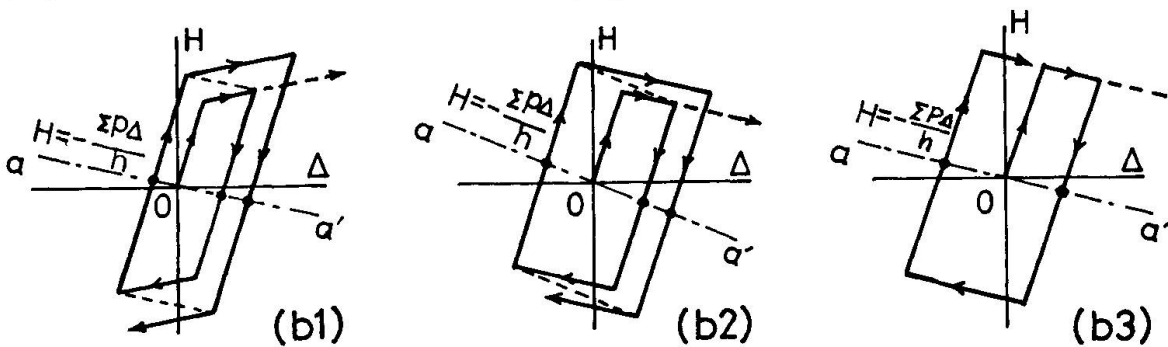
- (a) Vertical load  $P$  does not exist or are small. The positive range of  $H-\Delta$  curve are parallel to  $\Delta$ -axis, neglecting strain-hardening.
- (b) Vertical load  $P$  is large and hinges form at beam ends.  $H-\Delta$  curve is modeled by closed loop with negative gradient in plastic range.
- (c) Vertical load  $P$  is large and hinges form in columns.  $H-\Delta$  curve is modeled by helically expanding loops due to the accumulated compressive strains and strain hardening, with negative gradient in plastic range.

(FROM INTRODUCTORY REPORT ,THEME III,p.56, Fig.21)



(a) NO AXIAL LOAD

(b) WITH AXIAL LOAD



- (b1), (b2)----Moment capacity increases over  $M_p$  due to strain-hardening, and (b1), increasing rate overcomes  $P-\Delta$  effect.
- (b2),  $P-\Delta$  effect overcomes increasing rate.
- (b3)-----Moment capacity keeps  $M_p$  (no strain-hardening)
- (b4)-----Moment capacity decreases from  $M_p$  due to buckling etc..

(FROM PRELIMINARY REPORT,THEME I,p.27, Fig.9)

Leere Seite  
Blank page  
Page vide